Fragmentation and prethermal dynamical phases in disordered strongly interacting Floquet systems

Matthew Wampler and Israel Klich
Department of Physics, University of Virginia, Charlottesville, Virginia 22903, USA

(Received 25 January 2023; revised 7 September 2023; accepted 15 September 2023; published 25 September 2023)

We explore how disorder and interactions conspire in lattice models with sequentially activated hopping to produce K-body (or many-body) localized phases. Specifically, we show the rich variety of dynamics produced in the finely tuned interacting Floquet models considered recently [M. Wampler and I. Klich, SciPost Phys. **14**, 145 (2023)] is stabilized prethermally (or via many-body localization in some cases) in regions in parameter space near the special points where classical-like dynamics emerges. We also find additional parameter space regions where approximate classical-like behavior can occur away from the special Diophantine points and show how disorder may further stabilize them. Furthermore, the regions in parameter space where Hilbert space fragmentation occurs in the clean system (leading to Krylov subspaces exhibiting frozen dynamics, cellular automation, and subspaces exhibiting signs of ergodic behavior) may also be stabilized by the addition of disorder.

DOI: 10.1103/PhysRevB.108.104315

I. INTRODUCTION

Periodic driving of quantum systems has emerged as an exciting tool that may be used to engineer otherwise exotic behavior [1]. Furthermore, periodically driven (Floquet) systems may support phases that are forbidden in systems evolving under static Hamiltonians. Two prominent examples are discrete time crystals [2,3] and anomalous Floquet topological insulators [4–6]. Time crystals are a proposed phase [7] in which continuous time translation symmetry of a system is spontaneously broken (in analogy with the spontaneous breaking of spatial translation symmetry in the formation of crystal lattices). Following a no-go theorem for time crystals in static systems [8], it was discovered that it is possible for the discrete time translation symmetry in periodically driven systems to be spontaneously broken forming discrete time crystals [9]. Anomalous Floquet topological insulators take advantage of the inherently periodic nature of the noninteracting quasienergy spectrum of periodically driven systems to exhibit topological features in the band structure that are impossible for static systems. This anomalous band structure was realized in a model by Rudner-Lindner-Berg-Levin (RLBL) [10]. By adding a disordered onsite potential to the RLBL model, it was then found that the system supports a robust, new topological phase called the anomalous Floquet-Anderson topological insulator [4]. The physical manifestation of this exotic, topological band structure is the emergence of chiral edge modes existing alongside a fully localized bulk. Both discrete time crystals and the anomalous topological edge behavior of anomalous Floquet topological insulators have been realized across a variety of physical platforms [11–16].

A priori, it may be surprising that Floquet systems may exhibit robust phases since energy may be indefinitely absorbed from the drive, eventually leading to a featureless, infinite-temperature state [17–19]. However, this thermalization may be combated using three main mechanisms: (1) The driven system is connected to a reservoir, which acts as a heat sink, leading to nontrivial nonequilibrium steady states [20–23]. (2) Only systems where energy is absorbed exponentially slowly from the drive are considered, leading to a pseudostable "prethermal" phase [24–28]. (3) Disorder is added to the system, resulting in a localizing effect, that prevents thermalization. This phenomenon is referred to as many-body localization (MBL) [19,29–37] and is an interacting generalization of Anderson localization [38].

In constrained systems, there exists yet another route towards ergodicity breaking: Hilbert space fragmentation [39–42]. In this case, the full Hilbert space is broken into subspaces that evolve independently. This leads to cases where a system may have some Krylov subspaces that thermalize while others do not. When the size of the nonthermal Krylov subspaces scales polynomially with system size (i.e., only representing a measure zero portion of the full Hilbert space), the states in these subspaces are referred to as quantum many-body scars [40,43,44].

In this work, we consider a broad class of Floquet models where hoppings between neighboring pairs of sites are sequentially activated. A large number of Floquet systems that have received theoretical and/or experimental attention are contained within this class of models (e.g., [4–6,10,45–49]). A recent investigation [50] found that the dynamics of clean, interacting systems in this class of models may become exactly solvable for certain driving frequencies and interaction strengths. Specifically, these parameter values lead to evolution of Fock states into Fock states. The special points in parameter space where this occurs are found by solving an emergent set of Diophantine equations [51]. At other points in parameter space (also found via a set of Diophantine equations), the Hilbert space is fragmented into subspaces

supporting either frozen dynamics, classical cellular automation [52], or ergodic behavior.

Here, we add a disordered potential to the class of interacting, Floquet systems considered in [50]. We find that the disorder stabilizes, via K-body localization (described below) [53], the dynamics of systems perturbed away from the special, Diophantine points in parameter space, leading to robust phases. The exotic dynamics of these phases may include, for example, the spontaneous breaking of time translation symmetry to form discrete time crystals.

Furthermore, we find that there are other regions in parameter space, away from any special, Diophantine points, that also represent K-body localized phases. These regions are given by values of interaction strength and driving frequency that "almost" (see Sec. III) satisfy Diophantine conditions. In addition, at the points in the clean model where Hilbert space fragmentation occurs, the added disorder ensures that the frozen and cellular automation Krylov subspaces are stable to perturbations (in driving frequency and interaction strength) away from the special points in parameter space. In some cases the subspace is localized by the disorder. In other cases, the cellular automation dynamics of the subspace is stabilized over long timescales but is eventually expected to thermalize.

Note, the stability of our results hinges on K-body localization instead of the full many-body localization. K-body localization is a generalization of MBL where a system containing up to a maximum number of particles, K, is localized by disorder (thus MBL is given in the limit of $K \to \infty$). Unlike MBL, which has only been rigorously established in one dimension, K-body localization is established in generic dimensional systems [53]. However, K-body localized systems containing more than K particles will eventually be thermalized via $K+1$ particle correlations. Thus, in the thermodynamic limit, we expect our results describe the system prethermally [except for cases, especially in one dimension (1D), where full MBL may occur].

To help illustrate our results throughout this work, we will use a Hubbard interacting RLBL-like model on a square lattice. In addition to the model being particularly clear for expository purposes, it has also been the center of recent interest in [6] where it was found that the model supports a novel topological phase called a correlation-induced anomalous Floquet insulator (CIAFI). The phase is characterized by a hierarchy of topological invariants and supports quantized magnetization density. We describe how these results may be viewed from the perspective of this work and describe unique insights into the system that the Diophantine framework provides.

The rest of this paper is structured as follows. In Sec. II, we briefly review how Diophantine equations emerge in clean, periodically driven systems and their implications for the dynamics at special driving frequencies and interaction strengths (as described in [50]). In Sec. III, we perturbatively describe the evolution of these (so far clean) systems with parameter values close to the special, Diophantine points. Section IV describes how, once disorder is added, the evolution in this perturbative regime becomes K-body localized. For the example case of the Hubbard-RLBL model, we provide a phase diagram for where this localization occurs. Section V describes the stability of subspaces when Hilbert space fragmentation is weakly broken by perturbing away from points where a few (but not all) of the conditions for Fock state to Fock state evolution are satisfied. In Sec. VI, we corroborate the above results with numerical evidence. Finally, in Sec. VII we provide concluding remarks.

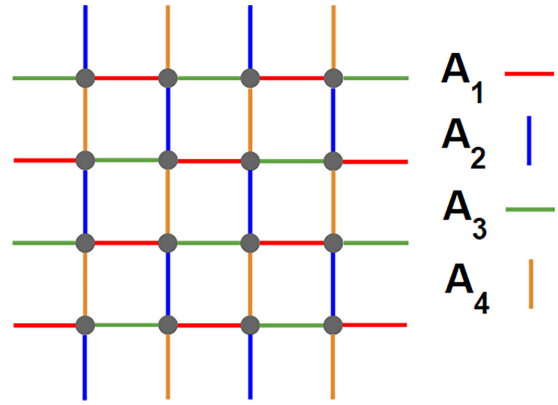

FIG. 1. The RLBL model. Hopping is sequentially activated among neighboring sites connected by the set A_m, $m = 1, \ldots, 4$.

II. INTERACTING FLOQUET MODELS, DIOPHANTINE EQUATIONS, AND HILBERT SPACE FRAGMENTATION

Here, we briefly review the identification of special evolution points following [50]. We look for conditions on fermion models to evolve Fock states into Fock states deterministically. We consider periodically driven models where hopping between neighboring sites is sequentially activated. Namely, we divide the period T of the Floquet drive into M steps where, during step m, particles are only allowed to hop between pairs of sites given by a set A_m. Interactions are then added to this free-hopping evolution, but we restrict ourselves to interactions that do not contain terms connecting two (or more) of the otherwise disjoint pairs with activated hopping. Specifically, evolution during the Floquet period $U(T)$ is given by

$$U(T) = U_M \ldots U_2 U_1, \tag{1}$$

where $U_m = e^{-i\tau \mathcal{H}_m}$, $\tau = \frac{T}{M}$, and

$$\mathcal{H}_m = -t_{\text{hop}} \sum_{(i,j)\in A_m;\sigma} (a^\dagger_{i,\sigma} a_{j,\sigma} + \text{H.c.}) + \mathcal{H}_{\text{int}}(\mathbf{V}_m), \tag{2}$$

where $\mathbf{V}_m$ is a set of interaction parameters. For the rest of this work, we will set $t_{\text{hop}} = 1$ unless otherwise noted.

As an example, consider the case of the RLBL model with Hubbard interactions. In this case, we set $M = 4$, choose A_m as given in Fig. 1, and set

$$\mathcal{H}^{\text{Hubbard}}_{\text{int}}(V) = V \sum_i n_{i,\uparrow} n_{i,\downarrow} \tag{3}$$

with $n_{i,\sigma} = a^\dagger_{i,\sigma} a_{i,\sigma}$. Note, the Hubbard interaction is onsite and thus leaves the pairs connected by A_m disjoint.

The next step is to find conditions for when individual, activated hopping pairs map Fock states into Fock states. Since the site pairs are disjoint, we may do this individually for each pair during each step m of the evolution.

In the Hubbard-RLBL model a two-site pair has 16 possible initial Fock states. Let us first consider the case of a single spin up at one site with an empty neighbor. We can ignore the interacting term, and compute directly the probability p for the particle to hop to site 2. We have

$$p = |\langle \text{vac}|a_2 e^{i\tau(a_1^\dagger a_2 + a_2^\dagger a_1)} a_1^\dagger |\text{vac}\rangle|^2 = \sin^2 \tau,$$

showing that when $\tau = \frac{\pi}{2}\ell$ with $\ell \in \mathbb{Z}$, the evolution maps this particular Fock state to a Fock state. Namely, the particle will remain at its initial site for τ with ℓ even and hop to the neighboring site when ℓ is odd. We repeat this procedure for the other 15 possible initial Fock states. The lines in the following table summarize the conditions we find on τ and V and the resulting type of evolution:

Particles	τ	V
1 or 3, frozen	$\frac{\pi}{2}\ell$, ℓ even	Arbitrary
1 or 3, swap	$\frac{\pi}{2}\ell$, ℓ odd	Arbitrary
2, opposite spins, frozen	$\frac{\pi}{2}\sqrt{2mn-n^2}$, n even	$\frac{4(n-m)}{\sqrt{2mn-n^2}}$
2, opposite spins, swap	$\frac{\pi}{2}\sqrt{2mn-n^2}$, n odd	$\frac{4(n-m)}{\sqrt{2mn-n^2}}$
Otherwise	Any	Any

(4)

where $\ell, m, n \in \mathbb{Z}$, and $2mn - n^2 > 0$. The left column refers to the number of particles in the initial state of the two-site pair (spin up + spin down) and the type of evolution we get. Thus, for example, if n is odd, and we start with a an up and down pair (a doublon) sitting at site 1, the doublon will hop to site 2. On the other hand, if n is even, the doublon will stay at site 1.

For a generic Fock state in the full system to evolve to another Fock state, we need every two-site activated pair to evolve deterministically. Hence, we require all the conditions in Eq. (4) to be satisfied simultaneously leading to a Diophantine equation [50].

It is also shown in [50] that, by solving the Diophantine equation, the following values of τ, V yield deterministic Fock state to Fock state evolution in the Hubbard-RLBL model:

$$\tau = \frac{\pi}{2} d\left(w_1^2 - w_2^2\right);\ V = \frac{8 w_1 w_2}{\left|w_1^2 - w_2^2\right|}, \tag{5}$$

where $w_1, w_2 \in \mathbb{Z}$, w_1, w_2 are coprime, and $d \in \frac{1}{\xi}\mathbb{Z}$ with $\xi = \gcd[(w_1^2 - w_2^2), (w_1^2 + w_2^2), (w_1 + w_2)^2]$. Below, we refer to the values of τ, V in (5) as Diophantine points.

Importantly, note that the analysis leading to Eq. (5) was independent of the fact that the driving procedure was RLBL. Thus, any periodic drive with sequentially activated hopping pairs, in any dimension, with Hubbard interactions will also exhibit deterministic Fock state to Fock state evolution at the special points in parameter space given by Eq. (5).

In summary, for each step m in the Floquet evolution, the evolution at a special, Diophantine point given by an evolution time τ_0 and a set of interaction parameters $\mathbf{V}_{0,m}$ is given by

$$U_m(\mathbf{V}_{0,m}, \tau_0) = \mathcal{P}_m, \tag{6}$$

where $\mathcal{P}_m$ is a complex permutation matrix on Fock states. A complex permutation matrix is a matrix where every row and column has a single nonzero element whose modulus is 1 (i.e., it is a permutation times a diagonal unitary). Furthermore, for local interactions, $\mathcal{P}_m$ deterministically updates the occupation of individual sites based on the occupation of neighboring sites. Starting from a product state, the evolution under an operator such as this, up to a phase, can be thought of as a classical cellular automation. It is for this reason that evolution such as this is sometimes referred to as "automation" dynamics [54].

What happens if only some of the conditions for Fock state to Fock state evolution are satisfied? In this case, the Hilbert space will fragment into subspaces. States in some subspaces will still evolve under cellular automation, while states in other subspaces are, in general, expected to ergodically explore their subspace.

For example, consider a Hubbard-Floquet model with a generic sequentially activated hopping. Like the Hubbard-RLBL model, the conditions for Fock state to Fock state evolution in this model are given by (4) [see discussion after Eq. (5)]. Now suppose only the fourth condition in (4) is satisfied (for example, $n = 3, m = 2$ with $\tau = \frac{\sqrt{3}}{2}\pi$ and $V = \frac{4\sqrt{3}}{3}$). This condition will state that an up-down pair at neighboring sites will swap spins. Therefore, the subspace of states with exactly one particle on each site (though the spin of each particle is left generic) is invariant under the evolution. Evolving any state in this subspace by U_m will still be equivalent to evolving it by $\mathcal{P}_m$ since there are no two-site activated pairs with 1 or 3 particles in the system. This implies that this exponentially large subspace will evolve as a classical process of spin swaps. On the other hand, Fock states that do have two-site pairs with 1 or 3 particles will evolve into superpositions of Fock states under U. For general hopping activation sequences, this leads to an ergodic exploration of the complementary subspace. The full Hilbert space is thus fragmented into independent subspaces exhibiting either cellular automation or ergodic evolution.

III. QUANTUM DYNAMICS IN SLOW MOTION

We now investigate how the systems considered in the previous section evolve when parameter values are perturbed away from the special, Diophantine points. In this case the evolutions U_m involved in the dynamics are no longer Fock state permutations. Rather, the evolution generates superpositions of Fock states and therefore entanglement.

We will show that when the perturbation is sufficiently small, the evolution during each Floquet period is given by the permutation associated with the special point, augmented with an evolution with an *effective local Hamiltonian* acting during a reduced time compared with the original evolution period. In other words, the correction to the classical cellular automation is a "slow motion" quantum dynamics.

We demonstrate the slowed behavior on several types of perturbations. For each perturbation type, we will present the form of the effective local Hamiltonian that emerges for the class of Floquet models represented by Eqs. (1) and (2). To further illustrate this effective slow dynamics, we then explicitly calculate the effective Hamiltonian for the Hubbard-RLBL model recounted in the previous section.

A. Perturbation in time

A simple perturbation to consider for a dynamical process is if the duration of evolution time steps is not precise. We therefore first consider a perturbation in the evolution time.

Consider a time τ_0, where the evolution step $U_m = e^{-i\tau_0\mathcal{H}_m} = \mathcal{P}_m$ is an exact permutation. If the duration τ_0 is shortened or lengthened to $\tau_0 + \delta\tau$, then we have the perturbed evolution

$$U_m(\mathbf{V}_{0,m}, \tau_0 + \delta\tau) = U_m(\mathbf{V}_{0,m}, \tau_0)U_m(\mathbf{V}_{0,m}, \delta\tau) \quad (7)$$

$$= \mathcal{P}_m e^{-i\delta\tau\mathcal{H}_m}. \quad (8)$$

In a process with M steps, each close to a permutation, the evolution of the full Floquet period is given by Eq. (1) as

$$U = \mathcal{P}_M e^{-i\delta\tau\mathcal{H}_M} \dots \mathcal{P}_2 e^{-i\delta\tau\mathcal{H}_2}\mathcal{P}_1 e^{-i\delta\tau\mathcal{H}_1}. \quad (9)$$

Defining the unperturbed permutation

$$\mathcal{P} = \mathcal{P}_M \dots \mathcal{P}_2\mathcal{P}_1,$$

and the nonpermutative correction to the dynamics U_{quantum} as

$$U_{\text{quantum}} = e^{-i\delta\tau\mathcal{P}_1^\dagger\mathcal{P}_2^\dagger\mathcal{P}_{M-1}^\dagger\mathcal{H}_M\mathcal{P}_{M-1}\dots\mathcal{P}_2\mathcal{P}_1} \dots \times e^{-i\delta\tau\mathcal{P}_1^\dagger\mathcal{H}_2\mathcal{P}_1}e^{-i\delta\tau\mathcal{H}_1}. \quad (10)$$

We have

$$U = \mathcal{P}U_{\text{quantum}}. \quad (11)$$

When tracking the evolution of a cluster of initial particles when the perturbation is small ($\delta\tau t_{\text{hop}}, \delta\tau V_{0,m} \ll 1$), it is convenient to think of the quantum correction as

$$U_{\text{quantum}} = e^{-i\delta\tau\mathcal{H}_{\text{eff}}},$$

where $\mathcal{H}_{\text{eff}}$ is given to lowest order in $\delta\tau$ as

$$\mathcal{H}_{\text{eff}} \simeq \sum_{m=1}^{M} \mathcal{P}_1^\dagger\mathcal{P}_2^\dagger \dots \mathcal{P}_{m-1}^\dagger\mathcal{H}_m\mathcal{P}_{m-1} \dots \mathcal{P}_2\mathcal{P}_1. \quad (12)$$

We note that as long as the range of each permutation $\mathcal{P}_m$ is finite, then the terms appearing in (12) will be local so long as each $\mathcal{H}_m$ is local. Moreover, the generation of superpositions of states is now governed by the slow timescale $\delta\tau$. This locality and slow development of superpositions will become important for arguments in Sec. IV.

Near points of frozen dynamics where $\mathcal{P}_m = I$, the correction U_{quantum} becomes the entire dynamics and, furthermore, from (12) we simply have $H_{\text{eff}} \simeq \sum H_m$. Let us again take as an example the Hubbard-RLBL model to further illustrate this slow-motion evolution governed by an effective local Hamiltonian. In this case, the vicinity of frozen dynamics is particularly simple and appealing. Here, the effective Hamiltonian becomes

$$H_{\text{eff}} = t_{\text{hop}} \sum_{(i,j);\sigma} (a_{i,\sigma}^\dagger a_{j,\sigma} + \text{H.c.}) + 4V_0 \sum_i n_{i,\uparrow}n_{i,\downarrow}, \quad (13)$$

which is the static Hubbard Hamiltonian on the square lattice with $V \to 4V_0$. This means that, to a good approximation, we may rewrite the evolution for a Floquet period T as $U(T) = e^{-iT\mathcal{H}_{\text{Floquet}}}$ with $\mathcal{H}_{\text{Floquet}} \simeq \frac{\delta\tau}{T}\mathcal{H}_{\text{Hubbard}}(4V_0)$. In other words, the stroboscopic evolution in the system is that of a slow-motion static Hubbard evolution, i.e., after N evolution cycles, at time TN, the system will have evolved under a static Hubbard Hamiltonian (with interaction $4V_0$) for a reduced time $\delta\tau N$.

We remark that when $\mathcal{P}_m \neq \mathbb{I}$, the evolution is a sequence of permutations followed by slowed, modified Hubbard evolution. In the Hubbard-RLBL case, only the hopping terms are modified by the permutations of lattice sites while the interaction terms are unaffected (since $\mathcal{H}_{\text{int}}^{\text{Hubbard}}$ counts the number of doublons, which is preserved under the freezing and swapping operations generating the dynamics at the special Diophantine points).

B. Perturbation in interaction strength

Now, suppose instead that we consider a perturbation in interaction parameters $\mathbf{V}_m = \mathbf{V}_{0,m} + \delta\mathbf{V}_m$. Here, $\delta\mathbf{V}_m$ is a vector of displacements to the set of interaction parameters $\mathbf{V}_{0,m}$ that correspond to one of the special points with permutative dynamics. In the case that $\tau_0\delta V_m \ll 1$ for all $\delta V_m \in \delta\mathbf{V}_m$, we expand

$$U_m(\mathbf{V}_{0,m} + \delta\mathbf{V}_m, \tau_0) \approx \mathcal{P}_m\left(1 - i\int_0^{\tau_0} ds\, e^{is\mathcal{H}_m(\mathbf{V}_{0,m})}\mathcal{H}_{\text{int}}(\delta\mathbf{V}_m)e^{-is\mathcal{H}_m(\mathbf{V}_{0,m})}\right)$$

defining

$$\mathcal{H}_{\text{eff},m} = \frac{1}{\tau_0}\int_0^{\tau_0} ds\, e^{is\mathcal{H}_m(\mathbf{V}_{0,m})}\mathcal{H}_{\text{int}}(\delta\mathbf{V}_m)e^{-is\mathcal{H}_m(\mathbf{V}_{0,m})}$$

we have

$$U_m(\mathbf{V}_{0,m} + \delta\mathbf{V}_m, \tau_0) \approx \mathcal{P}_m e^{-i\tau_0\mathcal{H}_{\text{eff},m}}. \quad (14)$$

Thus, in a similar fashion to the perturbation in τ case, we find that

$$U = \mathcal{P}_M \dots \mathcal{P}_2\mathcal{P}_1 e^{-i\tau_0\mathcal{H}_{\text{eff}}} \quad (15)$$

with

$$\mathcal{H}_{\text{eff}} \simeq \sum_{m=1}^{M} \mathcal{P}_1^\dagger\mathcal{P}_2^\dagger \dots \mathcal{P}_{m-1}^\dagger\mathcal{H}_{\text{eff},m}\mathcal{P}_{m-1} \dots \mathcal{P}_2\mathcal{P}_1. \quad (16)$$

Illustrating again with the Hubbard-RLBL model, $H_{\text{eff},m}$ may be written explicitly in terms of creation and annihilation operators by directly integrating $\int_0^{\tau_0} ds\, e^{is\mathcal{H}_m(\mathbf{V}_{0,m})}\mathcal{H}_{\text{int}}(\delta\mathbf{V}_m)e^{-is\mathcal{H}_m(\mathbf{V}_{0,m})}$. This may be done since each of the activated two-site hopping pairs are disjoint. Thus, we may solve separately for each two-site pair and then sum them all together, we find to lowest order in $\tau_0\delta V$ that

$$H_{\text{eff},m} = \delta V \sum_{i\in\text{2-site pairs}} n_{\leqslant\text{2-part},i}\mathbf{a}_i^\dagger\mathcal{T}\mathbf{a}_i n_{\leqslant\text{2-part},i} + n_{>\text{2-part},i}, \quad (17)$$

where we have defined

$$\mathcal{T} = \frac{-1}{16 + V_0^2}\begin{pmatrix} 12 - V_0^2 & -4 & V_0 & V_0 \\ -4 & 12 - V_0^2 & V_0 & V_0 \\ V_0 & V_0 & 4 & 4 \\ V_0 & V_0 & 4 & 4 \end{pmatrix}, \quad (18)$$

$$\mathbf{a}_i = (a_{2\uparrow}a_{2\downarrow} \quad a_{1\uparrow}a_{1\downarrow} \quad a_{1\uparrow}a_{2\downarrow} \quad a_{2\uparrow}a_{1\downarrow})^T \quad (19)$$

and $n_{>2\text{-part},i}$ projects onto the subspace with the ith two-site pair having more than two particles, i.e.,

$$n_{>2\text{-part}} = 1 - n_{\leqslant 2\text{-part}} = \sum_{\substack{a,b,c \in \{1\uparrow, 1\downarrow, 2\uparrow, 2\downarrow\} \\ a \neq b \neq c}} n_a n_b n_c. \quad (20)$$

In other words, evolution under $H_{\text{eff},m}$ corresponds to correlated hopping for any two-site pairs containing two particles and a δV energy cost of having a two-site pair with three or more particles.

C. Away from special points

Slowed effective quantum dynamics corrections to classical Fock state permutations may also occur away from the vicinity of the special Diophantine points. Here we explore other regions in parameter space, far from special points, where the conditions for Fock state to Fock state evolution are *approximately* satisfied. Specifically, consider the evolution at step m consisting of the set A_m of the activated two-site pairs, and let $\mathcal{H}_{(i,j)}$ be the Hamiltonian for $(i, j) \in A_m$.

Let us define

$$D_{(i,j)} = \inf_{\mathcal{P}_{(i,j)}} ||e^{-i\tau\mathcal{H}_{(i,j)}} - \mathcal{P}_{(i,j)}||_{\text{HS}} \; ; \; D = \max_{(i,j)} D_{(i,j)}, \quad (21)$$

where $||\cdot||_{\text{HS}}$ is the Hilbert-Schmidt norm of the (i, j) subspace. $\mathcal{P}_{(i,j)}$ is a complex permutation of Fock states within the two-site pair (i, j). When $D \ll 1$ we can say that the conditions for Fock state to Fock state evolution are approximately satisfied for $\mathcal{H}_m$ and τ.

We may now choose a $\mathcal{P}_{(i,j)}$ that minimizes $D_{(i,j)}$ and write

$$e^{-i\tau\mathcal{H}_{(i,j)}} \equiv \mathcal{P}_{(i,j)} e^{-i\tau\mathcal{H}_{\text{eff},(i,j)}}. \quad (22)$$

It follows that $e^{-i\tau\mathcal{H}_{\text{eff},(i,j)}}$ is close to the identity matrix when D is small, therefore, the evolution corresponds to a permutation augmented with slowed quantum dynamics. Using Eq. (22) the evolution of the full system for step m is

$$U_m = \bigotimes_{(i,j)\in A_m} e^{-i\tau\mathcal{H}_{(i,j)}} = \mathcal{P}_m e^{-i\tau\mathcal{H}_{\text{eff},m}}, \quad (23)$$

where we have defined

$$\mathcal{P}_m = \bigotimes_{(i,j)\in A_m} \mathcal{P}_{(i,j)}, \quad (24)$$

$$\mathcal{H}_{\text{eff},m} = \sum_{(i,j)\in A_m} \mathcal{H}_{\text{eff},(i,j)}. \quad (25)$$

Equation (23) has the same general form as Eqs. (14) and (8), and we find analogously that the evolution of the full Floquet period is again given by (15) and (16).

To illustrate the appearance of slow dynamics parameter space regions away from special points, in Fig. 2 we plot regions where the Diophantine conditions are approximately satisfied in the Hubbard-RLBL model. Namely, we plot regions where the Hilbert-Schmidt norm of the difference between the evolution of an activated pair and a SWAP or identity permutation is less than some small cutoff ($D_{(i,j)} < 0.1$). We further note that, since the Hamiltonian $\mathcal{H}_{(i,j)}$ is particle number preserving, we may consider separately the cases where the pair (i, j) contains $0, 1, 2, 3,$ or 4 particles. In other words, we may analyze a separate $D^{(a)}_{(i,j)}$ for each of the particle-number subspaces $a \in \{0, 1, 2, 3, 4\}$, with $\sum_a D^{(a)}_{(i,j)} = D_{(i,j)}$. In the Hubbard-RLBL model, evolution of a pair with 0 or 4 particles is trivially the identity by Pauli exclusion (i.e., $D^{(a)}_{(i,j)} = 0$ in these subspaces). Furthermore, evolution of a two-site pair with a single particle is equivalent to the evolution of a hole in a two-site pair with three particles. Thus, $D^{(1)}_{(i,j)} = D^{(3)}_{(i,j)}$. In Fig. 2, we therefore plot when $D^{(1)}_{(i,j)}$ and when $D^{(2)}_{(i,j)}$ are smaller than the cutoff. We refer to these as the single-particle and doublon sectors, respectively. We also use a color code to differentiate which permutation $\mathcal{P}^{(a)}_{(i,j)}$ of the pair (i, j) within the subspace a minimizes $D^{(a)}_{(i,j)}$. Specifically, parameters where pairs with one or three particles are approximately frozen (perfect swapping) are colored green (yellow) while parameters where pairs with two particles of opposite spin[1] are approximately frozen (perfect swapping) are colored blue (red). Thus, $D_{(i,j)}$ (and subsequently, D) is small only in regions of overlapping colors. Note that each special, Diophantine point is surrounded by a region of overlapping colors, but not all regions of overlapping colors contain a special point.

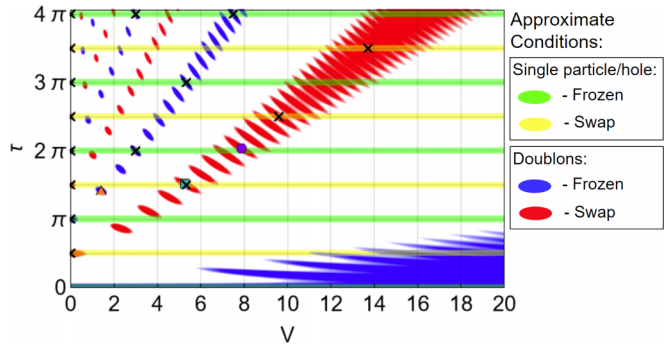

FIG. 2. Parameter space regions where the Diophantine conditions (4) are approximately satisfied. The special, Diophantine points where evolution is exactly a Fock state permutation are marked with a black "X." Also plotted are the points numerically investigated in Fig. 3.

A couple of remarks are in order. Note that in the Hubbard-RLBL model, special points are only found when all activated two-site pairs are frozen or when all the pairs are perfect swapping (see [50]). Indeed, in Fig. 2 the special points (represented by x) appear only when both single-particle and doublon sectors are simultaneously perfectly swapping (or simultaneously perfectly frozen). However, Fig. 2 also shows that it is possible to approximately have perfect swapping in the one- and three-particle sector while pairs with two particles are approximately frozen (and vice versa).

Another thing to note is that when only some of the Diophantine conditions are approximately satisfied, the fragmented Krylov subspaces that would emerge if the conditions were perfectly satisfied may become connected by the slowed

[1]If the two particles have the same spin, the evolution is trivially the identity by Pauli exclusion.

dynamics $\mathcal{H}_{\text{eff}}$. We remark further on the importance of this in Sec. V.

We note that an alternative measure for how far the evolution is from permutative is presented in [50], based on the function

$$F_{p,q}(U) = -\log \frac{||U||_{p,q}}{\dim(U)^{1/q}} = -\frac{1}{q}\log \frac{\sum_{n,m}|U_{n,m}|^p}{\dim(U)} \tag{26}$$

defined on unitary matrices where $\dim(U)$ is the dimensionality, and $||U||_{p,q} = (\sum_{n,m}|U_{n,m}|^p)^{1/q}$ is the p,q matrix entrywise norm. It is straightforward to check that for $p > 2, q > 0$, the function F reaches its minimum $F_{p,q}(U) = 0$ if and only if U is a complex permutation matrix. However, in Fig. 2 we wanted to distinguish between the different types of permutative behavior (frozen vs perfect swapping) and so instead focused on using (21).

In the next section, we add disorder to the system and find that the slowed dynamics is (in some cases) either K-body or many-body localized by the disorder. This then stabilizes the cellular automation dynamics in regions where the conditions for Fock state to Fock state evolution are approximately satisfied leading to robust phases.

IV. STABILIZING CLASSICAL EVOLUTION WITH DISORDER

We now add disorder to the periodically driven, interacting models considered above. Specifically, we investigate Floquet drives of the form

$$U(T) = U_{\text{dis}}U_M \dots U_2U_1, \tag{27}$$

where we take U_{dis} to be evolution under a disordered onsite potential with no hopping, i.e.,

$$U_{\text{dis}} = e^{-i\tau\mathcal{H}_{\text{dis}}}, \tag{28}$$

where

$$\mathcal{H}_{\text{dis}} = \sum_{i,\sigma} v_i n_{i,\sigma} \tag{29}$$

with v_i uniformly distributed in $[-W, W]$. However, the exact form of disorder does not play a role in the argument.[2]

For Floquet systems of this type, sufficiently strong disorder will (either K-body or many-body) localize the slowed dynamics but leave the cellular automation dynamics unaffected. This happens when the Fock state permutation has a finite order and when the disorder is large compared to the slowed evolution. This leads to the emergence of robust phases with stabilized permutative dynamics.

A. Dynamics with disorder close to $\mathcal{P} = I$

To illustrate how this occurs, we begin with the simpler case of when the permutation of the full Floquet period (though not necessarily each step m of the drive) is the identity, i.e.,

$$\mathcal{P}_M \dots \mathcal{P}_2\mathcal{P}_1 \equiv \mathcal{P} = I, \tag{30}$$

where $\mathcal{P}$ is the permutation associated with a full Floquet period. Examples with permutations of this type include frozen dynamics and the perfect swapping Hubbard-RLBL model with periodic boundary conditions (e.g., $\tau = \frac{\pi}{2}$, $V = 0$ or $\tau = \frac{3\pi}{2}, V = \frac{16}{3}$).

Using (15) we find that, for parameters where the Diophantine conditions are approximately satisfied, the evolution of one Floquet period T may be written

$$\begin{aligned} U &= U_{\text{dis}}\mathcal{P}e^{-i\tau\mathcal{H}_{\text{eff}}} && (31)\\ &= U_{\text{dis}}e^{-i\tau\mathcal{H}_{\text{eff}}} && (32)\\ &\approx U_{\text{dis}}\left(1 - i\int_0^\tau dt\, e^{it\mathcal{H}_{\text{dis}}}\mathcal{H}_{\text{eff}}(t)e^{-it\mathcal{H}_{\text{dis}}}\right) && (33)\\ &= \mathcal{T}e^{-i\int_0^\tau dt\,\mathcal{H}(t)}, && (34)\end{aligned}$$

where

$$\mathcal{H}_{\text{eff}}(t) = e^{-it\mathcal{H}_{\text{dis}}}\mathcal{H}_{\text{eff}}e^{it\mathcal{H}_{\text{dis}}}, \tag{35}$$

$$\mathcal{H}(t) = \mathcal{H}_{\text{dis}} + \mathcal{H}_{\text{eff}}(t). \tag{36}$$

Therefore, in order to show that the permutation (in this case $\mathcal{P} = I$) is stable, we must show that the Hamiltonian (36) is localized.

To see when this is the case, we rewrite (36) as

$$\mathcal{H}(t) = \mathcal{H}^{(0)} + V(t), \tag{37}$$

where

$$\mathcal{H}^{(0)} = \mathcal{H}_{\text{dis}} + \overline{\mathcal{H}_{\text{eff}}(t)}, \tag{38}$$

$$V(t) = \mathcal{H}_{\text{eff}}(t) - \overline{\mathcal{H}_{\text{eff}}(t)};\ \overline{V(t)} = 0 \tag{39}$$

with $\overline{f(t)} = \frac{1}{\tau}\int_0^\tau ds\, f(s)$ the time average and $V(t)$ is the strictly time-dependent part of $\mathcal{H}(t)$.

We note that $\mathcal{H}_{\text{eff}}$ is a sum of local Hamiltonians sandwiched by $\mathcal{P}_m$ [Eq. (16)] and is thus also local. This implies that $V(t)$ is local as well and may be written

$$V(t) = \sum_i V_i(t). \tag{40}$$

Whenever $\mathcal{H}^{(0)}$ is MBL, we may use a theorem by Abanin, De Roeck, and Huveneers [35] to show that the weak, local drive $V(t)$ will not ruin the localization of $\mathcal{H}^{(0)}$. Namely, that the Hamiltonian (36) will be MBL whenever

$$\tau||V_i(t)||_{\text{HS}} \ll 1 \text{ and } \frac{\tau||V_i(t)||^2_{\text{HS}}}{W} \ll 1. \tag{41}$$

Note that $\tau||\mathcal{H}_{\text{eff},i}||_{\text{HS}} \ll 1$ implies $\tau||V_i(t)||_{\text{HS}} \ll 1$. Hence, for sufficiently strong disorder, the Hamiltonian (36) will be MBL so long as $\mathcal{H}^{(0)}$ is MBL. A corollary of this result is that (36) will be K-body localized so long as $\mathcal{H}^{(0)}$ is K-body localized.[3]

[2]Note, for example, if H_{dis} is included as a constant term throughout the evolution instead of only being applied during the U_{dis} portion of the drive, then all our results still hold [6]. In this case, the strength of the disorder during the first four steps of the Floquet drive must be kept small. The strength during the fifth, disorder only, step may be made large by lengthening the time that U_{dis} is applied.

[3]This is because [35] uses a KAM-type scheme to, order by order, find exactly the dressed ℓ bits of the Hamiltonian and thus prove it is MBL. This procedure may thus be stopped at some order K to show K-body localization.

We have thus reduced the problem to asking whether the static Hamiltonian $\mathcal{H}^{(0)}$ is localized. For 1D systems, we expect $\mathcal{H}^{(0)}$ to be MBL. This is because, using a Kolmogorov-Arnold-Moser (KAM)-type scheme, it has been shown that models of this type (i.e., Hamiltonians with a disordered term plus a weak, local interacting term) are MBL in 1D under the weak assumption of limited level attraction (see [34]). In higher dimensions, rare regions of weak disorder can cause an avalanche effect that ruins the MBL [55–58]. This delocalization, however, happens on exponentially long timescales and thus the system is prethermally localized. Furthermore, these systems are expected to be K-body localized. This is because the probability that the K-particle energy spectrum features the accidental resonances that ruin localization goes to zero in the thermodynamic limit [53].

In summary, we have shown that when disorder is added to a Floquet system near a special point with $\mathcal{P} = I$, then the dynamics is stabilized by (many-body or K-body) localization and thus corresponds to a robust prethermal phase. We expect that as we move further away from special points, the effective evolution would resemble that of random local unitaries in which spreading has been studied in, e.g., [59].

B. Discrete time crystals

We now consider a Floquet drive that corresponds to a perfect cellular automation with some finite order $\geqslant 1$, i.e.,

$$\mathcal{P}^{\mathcal{O}} = I;\ \mathcal{O} \in \mathbb{N}. \tag{42}$$

Such dynamics, when stable to disorder and $\mathcal{O} > 1$, is often called a discrete time crystal. Indeed, the original time translation symmetry of the Floquet drive T has been spontaneously broken in these interacting, localized Floquet phases that now have $\mathcal{O}T$ time translation symmetry. Let us consider the evolution after $\mathcal{O}$ Floquet periods given by

$$U^{\mathcal{O}} = [U_{\text{dis}}\mathcal{P}e^{-i\tau\mathcal{H}_{\text{eff}}}]^{\mathcal{O}} \tag{43}$$

$$= [U_{\text{dis}}\mathcal{P}]^{\mathcal{O}}e^{-i\tau\mathcal{H}_{\mathcal{O},\text{eff}}}, \tag{44}$$

where, to first order in $\tau||\mathcal{H}_{\text{eff},(i,j)}||_{\text{HS}}$,

$$\mathcal{H}_{\mathcal{O},\text{eff}} = \sum_{a=0}^{\mathcal{O}-1}(\mathcal{P}^{\dagger}U_{\text{dis}}^{\dagger})^{a}\mathcal{H}_{\text{eff}}(U_{\text{dis}}\mathcal{P})^{a}. \tag{45}$$

Now, note that since $\mathcal{P}$ is a cellular automation (and thus updates the occupancy of sites based on the occupancy of nearby sites), it transforms the number operator of a site i in the following way:

$$\mathcal{P}^{\dagger}n_i\mathcal{P} = \sum_{i_1} P_{i_1}n_{i_1} + \sum_{i_1,i_2} P_{i_1i_2}n_{i_1}n_{i_2} + \cdots + \sum_{i_1,i_2,\ldots,i_\lambda} P_{i_1i_2\ldots i_\lambda}n_{i_1}n_{i_2}\ldots n_{i_\lambda}, \tag{46}$$

where the coefficients $P_{i_1}, P_{i_1i_2}, \ldots, P_{i_1i_2\ldots i_\lambda}$ are only nonzero when all the sites $i_1, i_2, \ldots, i_\lambda$ are within some finite region surrounding site i. This implies that

$$[U_{\text{dis}}\mathcal{P}]^{\mathcal{O}}e^{-i\tau\mathcal{H}_{\mathcal{O},\text{eff}}} = \mathcal{P}^{\mathcal{O}}e^{-i\tau\mathcal{H}_{\text{loc}}}e^{-i\tau\mathcal{H}_{\mathcal{O},\text{eff}}} = e^{-i\tau\mathcal{H}_{\text{loc}}}e^{-i\tau\mathcal{H}_{\mathcal{O},\text{eff}}}, \tag{47}$$

where

$$\mathcal{H}_{\text{loc}} = \sum_{a=0}^{\mathcal{O}-1}\mathcal{P}^{a}\mathcal{H}_{\text{dis}}\mathcal{P}^{a}. \tag{48}$$

Note that $\mathcal{H}_{\text{loc}}$ is a sum of local terms as in (46). We now repeat the steps (32) to (37) to find that

$$U^{\mathcal{O}} = \mathcal{T}e^{-i\int_0^\tau dt\,\mathcal{H}(t)} \tag{49}$$

with

$$\mathcal{H}(t) = \mathcal{H}^{(0)} + V(t) \tag{50}$$

and

$$\mathcal{H}^{(0)} = \mathcal{H}_{\text{loc}} + \overline{\mathcal{H}_{\mathcal{O},\text{eff}}(t)}, \tag{51}$$

$$V(t) = \mathcal{H}_{\mathcal{O},\text{eff}}(t) - \overline{\mathcal{H}_{\mathcal{O},\text{eff}}(t)}, \tag{52}$$

$$\mathcal{H}_{\mathcal{O},\text{eff}}(t) = e^{-it\mathcal{H}_{\text{loc}}}\mathcal{H}_{\mathcal{O},\text{eff}}e^{it\mathcal{H}_{\text{loc}}}. \tag{53}$$

Again using [35], we find that (50) is K-body (many-body) localized whenever $\mathcal{H}^{(0)}$ is K-body (many-body) localized and (41) are satisfied. Again, since $\mathcal{H}^{(0)}$ is a fully MBL term plus a weak, local interacting term, we expect it to be K-body (many-body) localized as discussed in the paragraph following (41).

We remark that the range of $\mathcal{H}_{\mathcal{O},\text{eff}}$, and thus $||V_i(t)||_{\text{HS}}$, increases with increasing $\mathcal{O}$. By (41), this implies that the region in parameter space where the system is localized will shrink rapidly for increasing $\mathcal{O}$, however, the region will remain finite so long as $\mathcal{O}$ is finite. This also suggests that general cellular automations without finite order are not likely to be stabilized by the disorder. For example, for the perfect swapping RLBL model, the bulk permutation has order 1 while the permutation at the edge has infinite order (since particles are transported chirally along the edge). This is another way of viewing why the edge modes of an interacting, perfect-swapping RLBL model thermalize [5,6] even while the system with periodic boundary conditions does not.

V. STABILIZED SUBSPACES

We now investigate when interacting models with sequentially activated hopping may exhibit stabilized permutative dynamics in Krylov subspaces even when the full Hilbert space does not support such dynamics. Namely, we consider two main situations where this may occur.

First, we can have all the Diophantine conditions approximately satisfied, but the corresponding permutation has infinite order when acting on some states (e.g., edge states in the RLBL model). However, some initial Fock states may exhibit finite orbits under the cellular automation (we give such an example using the Hubbard-RLBL model later in this section). As we will soon show, these orbits may then be stabilized by disorder.

Another possibility is when only some of the Diophantine conditions are approximately satisfied. Here, the Hilbert space fragmentation (that occurs when a few of the Diophantine

conditions are perfectly satisfied [50]) may be stabilized by the disorder.

In both these cases, we are thus interested in Floquet evolution that may be written

$$U(T) = U_{\text{dis}} U_{\mathcal{P}} e^{-i\tau \mathcal{H}_{\text{eff}}}. \tag{54}$$

Here $U_{\mathcal{P}}$ maps number states to number states only in a subspace $\mathcal{N}$ associated with satisfied conditions. Let us consider cases where

$$U_{\mathcal{P}}^{\mathcal{O}} |\mathcal{N}\rangle = |\mathcal{N}\rangle \tag{55}$$

for some finite $\mathcal{O} \in \mathbb{N}$.

We now ask whether the subspace $\mathcal{N}$ is localized under the evolution $U(T)$. We first specialize to the situation where the subspace $\mathcal{N}$ is closed under the evolution of $U(T)$, i.e.,

$$U(T)|\mathcal{N}\rangle = |\mathcal{N}'\rangle \ \ \forall \ \ |\mathcal{N}\rangle \in \mathcal{N}, \tag{56}$$

where $|\mathcal{N}'\rangle \in \mathcal{N}$. A simple example when this (approximately) happens is when starting with a few particles far away from the edge in the RLBL model. A more elaborate example will be discussed below.

When $\mathcal{N}$ is closed under the evolution, $U(T)$ is block diagonal with

$$U(T) = \begin{pmatrix} U_{\mathcal{N}^c} & 0 \\ 0 & U_{\mathcal{N}} \end{pmatrix}, \tag{57}$$

where $U_{\mathcal{N}}$ acts on the space $\mathcal{N}$ and $U_{\mathcal{N}^c}$ acts on its complement $\mathcal{N}^c$.

Now, using (54) and (55) and repeating the steps (43) through (49), we have that $U_{\mathcal{N}}^{\mathcal{O}}$ is localized.

We again illustrate our point using the Hubbard-RLBL model. Consider the case where activated pairs with one or three particles are approximately perfect swapping while pairs with two particles of opposite spin are approximately frozen (i.e., regions in Fig. 2 where yellow and blue overlap). Here, the corresponding cellular automation has infinite order. However, the cellular automation does have finite order when acting on subspaces with a fixed, finite number of particles. Furthermore, note that the Hubbard-RLBL evolution is U(1) symmetric, thus the finite particle number subspaces are closed under $U(T)$. Therefore, by the arguments of this section, we have that the cellular automation will be stabilized by disorder for any initial state with a fixed, finite number of particles.

For cases where the subspace $\mathcal{N}$ is not closed under the evolution $U(T)$ it might be expected, in general, that the system will fail to localize. This is because, as soon as the initial state evolves outside the subspace $\mathcal{N}$, the operator $U_{\mathcal{P}}$ will act to delocalize the state. However, we investigate such cases numerically in the next section and find that initial states within $\mathcal{N}$ may still remain localized on prethermal timescales.

VI. NUMERICAL RESULTS

In this section, we numerically investigate the evolution of several example interacting Floquet systems both with and without disorder. Namely, we investigate the stabilizing effect when disorder is added and if the evolution is consistent with localization dynamics.

As a measure of localization, we use the inverse participation ratio (IPR). Given any state $|\Psi\rangle$, and letting $|\mathbf{n}\rangle$ be the number-state basis in real space, the IPR is defined as

$$\text{IPR} = \sum_{\mathbf{n}} |\langle \Psi | \mathbf{n} \rangle|^4. \tag{58}$$

The IPR is 1 for any $|\Psi\rangle$ that is a Fock state and goes as $\frac{1}{N^2}$ (where N is the dimension of the Hilbert space) for an equal superposition of number states.

In Fig. 3(a), we plot the IPR as a function of time for three example values of V, τ in the Hubbard-RLBL model starting from the initial Fock state of a doublon localized in the center of the system.

In the first case, the second and fourth conditions in (4) are approximately satisfied with $V = \frac{16}{3} - 0.05$, $\tau = \frac{3\pi}{2} + 0.05$, i.e., we have perturbed both V, τ away from the special point $V = \frac{16}{3}, \tau = \frac{3\pi}{2}$ where both single particles and doublons evolve with swapping. Without disorder, the system will evolve with the effective slowed, interacting dynamics as discussed in Sec. III since it is near a special point. However, the doublon under this dynamics may still generate superpositions and spread throughout the system. Thus, the IPR decreases. Note, however, that the Fock state permutation at the special, Diophantine point has finite order (namely, order 1 since the perfect swapping RLBL model acts as the identity in the bulk of the system). Therefore, by the analysis of Sec. IV, it is expected that disorder will K-body (in this case, two-body) localize the evolution. Consistent with this result, it can be seen in Fig. 3(a) that the IPR approaches a constant value ($\sim$0.8) when disorder is included. In Fig. 3(b), the average density of spin-up particles[4] at each site is plotted after 10 000 Floquet periods. Without disorder, the particle spreads throughout the entire system. With disorder, it remains localized around its initial location.

In the second case, we evolve under Hubbard-RLBL with the parameters $V = 7.9$, $\tau = 2\pi + 0.1$. This point in parameter space is not in the vicinity of any Diophantine points, but, nonetheless, the first and fourth conditions (single particles frozen, doublons swapping) in (4) are approximately satisfied (since the point is in an overlapping red and green region in Fig. 2). Similar to the first case, the evolution without disorder exhibits slowed, effective dynamics with the IPR decreasing over time [Fig. 3(a)]. When disorder is added, the IPR again converges to a constant value ($\sim$0.8). Note, the Fock state permutation corresponding to single particles frozen and doublons swapping does not have finite order. However, it does have finite orbits in the two-particle subspace, and, furthermore, the evolution is U(1) symmetric. Thus, evolution is confined to the two-particle subspace. This implies that, consistent with the numerics, disorder is again expected to localize the system by the arguments of Sec. V.

In the third case, we consider evolution at $V = \sqrt{2} - 0.01$, $\tau = \sqrt{2}\pi + 0.01$. Here, only the third condition in (4) is approximately satisfied (doublons frozen). If the third condition

[4]Due to the up-down symmetry of the evolution, the average density of spin-down particles is equivalent to the average density of spin-up particles and thus the spin-down density plots are not included.

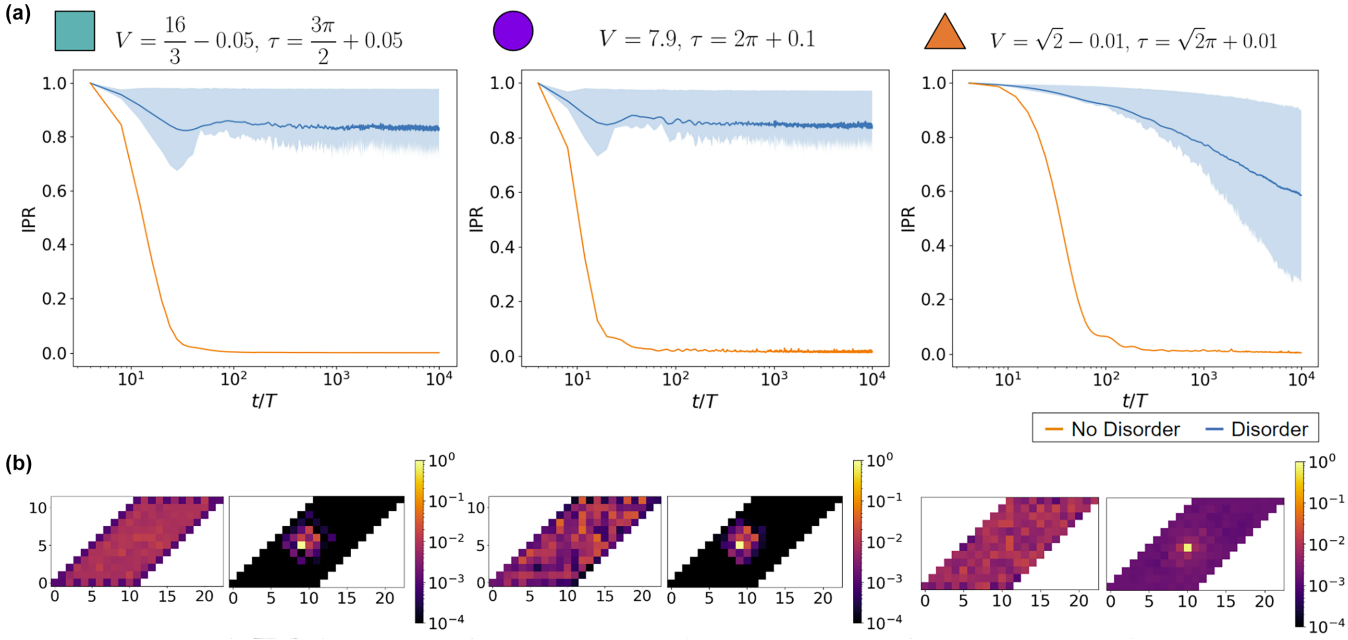

FIG. 3. Localization in Hubbard-RLBL: (a) Evolution of the inverse participation ratio (IPR) in the Hubbard-RLBL model for a doublon initially localized in the center of the system when disorder either is or is not present. From left to right, the figures correspond to the second and fourth conditions in (4) being approximately satisfied (both particles and doublons are swapping), the first and fourth conditions being approximately satisfied (particles are frozen and doublons are swapping), and solely the third condition being approximately satisfied (doublons are frozen). The location of each example in parameter space is plotted in Fig. 2. Disordered runs are averaged over 500 realizations of $W = 10$ with the range from the 25th to the 75th percentiles filled in with light blue. Consistent with the theoretical arguments of Secs. IV and V, the numerics suggest that disorder fully localizes the evolution in the first two cases and stabilizes the classical dynamics over exponentially long timescales in the third case. (b) Average density of spin-up particles per site after 10 000 driving periods from an initial doublon localized in the center of the system. For each value of V, τ, the densities after evolution without disorder (left) and with disorder (right) are plotted.

was exactly satisfied, the Hilbert space fragments leaving any configuration of doublons frozen while other particle configurations may thermalize. However, since the third condition is only approximately satisfied, doublons have a small chance to separate into a spin-up and -down particle. This was not a problem in cases 1 and 2 as the dynamics of single particles was also approximately permutative, implying that each of the single particles from the split doublon would continue to exhibit localized dynamics on their own in the presence of disorder. In contrast, the single-particle dynamics is delocalized in this case, even in the presence of disorder. Thus, as soon as a doublon splits, the resulting pair of single particles will delocalize the system. In the language of Sec. V, the perturbation allows the system to evolve out of the Fock state permutation subspace and disorder is not guaranteed to localize the evolution. This is reflected in Fig. 3(a) where the IPR no longer converges once disorder is added. However, the disorder does help to stabilize the frozen dynamics of the doublon over long timescales. The difference from the first two cases is also apparent when considering the average particle density Fig. 3(b). Here, the doublon is still with high probability localized near its initial location, but once it splits (thereby leaving the frozen subspace) the single particles may travel throughout the system. This creates a nonzero background in the average particle density even far from the initial doublon location.

VII. SUMMARY AND DISCUSSION

In this work, we have shown that interacting Floquet models with periodically activated pairs exhibit classical cellular automation dynamics corrected by a slowed, effective interacting evolution when a given set of conditions [e.g., (4)] are approximately satisfied. Furthermore, when disorder is added to the system, these regions with approximately satisfied conditions become robust prethermal phases. If only a few of the Diophantine conditions are satisfied, the Hilbert space fragments into cellular automation subspaces and ergodic subspaces. When the same conditions are instead approximately satisfied, the disorder stabilizes the dynamics in the cellular automation subspace for long, but not infinite, timescales. On the other hand, these subspaces may still support localization if the subspace is closed under the evolution.

The existence of these stabilized cellular automation phases opens the door to a systematic investigation into their properties. For example, in [6] the disordered Hubbard-RLBL model was investigated at $\tau = \frac{\pi}{2}$ with V approaching 0 and V approaching infinity. It was found that, in this regime, the system belongs to a class of anomalous Floquet topological insulators, called correlation-induced anomalous Floquet insulators (CIAFI), labeled by a hierarchy of topological invariants. The two different values of V correspond to topological insulators with two differing topological invariants. From the perspective of our work, this corresponds to the

cases where single particles and doublons are approximately swapping (conditions two and four approximately satisfied) for V near 0 and correspond to single particles swapping and doublons frozen (conditions two and three approximately satisfied) for V large. Thus, any parameter space region with those Diophantine conditions approximately satisfied will also correspond to a CIAFI with the corresponding topological invariants. Similarly, when other Diophantine conditions are approximately satisfied, we expect the system to again correspond to a CIAFI with different topological invariants. This is just one example of the interesting phenomena that may occur in systems with stabilized cellular automation dynamics and an exciting direction for future work is the investigation of possible exotic behavior found in systems stabilizing other cellular automata. For example, it would be interesting to consider interacting Floquet drives without U(1) symmetry such that the corresponding cellular automation may not preserve particle number.

One restriction used in this work to show localization was the finite order of the cellular automation. It is an open question as to whether there are any systems where this constraint may be relaxed. Another interesting possibility is the generalization of the models discussed in this work to aperiodically driven systems. If this is possible, the prospective stabilized cellular automation corresponding to the evolution of such a drive would necessarily be aperiodic as well and therefore allow for more general stabilized cellular automata. Recent work has suggested the existence of prethermal phases for aperiodically driven systems [60,61].

Instead of periodic drives, it is also possible to restrict hopping to between pairs of sites via measurements. Recently, it was shown that, in this way, it is possible to mimic the RLBL procedure to produce protected edge transport alongside a local bulk via measurements alone [62]. Due to the nonunitary nature of the measurements, the analysis in this paper does not directly apply in the measurement-induced setting. A possible avenue for future investigations is determining if the stabilized cellular automation dynamics is also possible for measurement-induced systems and, if so, what similarities and differences does the dynamics have with the Floquet systems considered here.

ACKNOWLEDGMENTS

Our work was supported in part by the NSF Grant No. DMR-1918207. I.K. thanks O. Motrunich for discussions.

[1] M. S. Rudner and N. H. Lindner, Band structure engineering and non-equilibrium dynamics in floquet topological insulators, Nat. Rev. Phys. **2**, 229 (2020).

[2] D. V. Else, C. Monroe, C. Nayak, and N. Y. Yao, Discrete time crystals, Annu. Rev. Condens. Matter Phys. **11**, 467 (2020).

[3] K. Sacha, *Time Crystals*, *Springer Series on Atomic, Optical, and Plasma Physics*, 1st ed. (Springer, Cham, 2021).

[4] P. Titum, E. Berg, M. S. Rudner, G. Refael, and N. H. Lindner, Anomalous Floquet-Anderson Insulator as a Nonadiabatic Quantized Charge Pump, Phys. Rev. X **6**, 021013 (2016).

[5] F. Nathan, D. Abanin, E. Berg, N. H. Lindner, and M. S. Rudner, Anomalous floquet insulators, Phys. Rev. B **99**, 195133 (2019).

[6] F. Nathan, D. A. Abanin, N. H. Lindner, E. Berg, and M. S. Rudner, Hierarchy of many-body invariants and quantized magnetization in anomalous Floquet insulators, SciPost Phys. **10**, 128 (2021).

[7] F. Wilczek, Quantum Time Crystals, Phys. Rev. Lett. **109**, 160401 (2012).

[8] H. Watanabe and M. Oshikawa, Absence of Quantum Time Crystals, Phys. Rev. Lett. **114**, 251603 (2015).

[9] D. V. Else, B. Bauer, and C. Nayak, Floquet Time Crystals, Phys. Rev. Lett. **117**, 090402 (2016).

[10] M. S. Rudner, N. H. Lindner, E. Berg, and M. Levin, Anomalous Edge States and the Bulk-Edge Correspondence for Periodically Driven Two-Dimensional Systems, Phys. Rev. X **3**, 031005 (2013).

[11] J. Zhang, P. W. Hess, A. Kyprianidis, P. Becker, A. Lee, J. Smith, G. Pagano, I.-D. Potirniche, A. C. Potter, A. Vishwanath, N. Y. Yao, and C. Monroe, Observation of a discrete time crystal, Nature (London) **543**, 217 (2017).

[12] P. Frey and S. Rachel, Realization of a discrete time crystal on 57 qubits of a quantum computer, Sci. Adv. **8**, eabm7652 (2022).

[13] Y.-G. Peng, C.-Z. Qin, D.-G. Zhao, Y.-X. Shen, X.-Y. Xu, M. Bao, H. Jia, and X.-F. Zhu, Experimental demonstration of anomalous floquet topological insulator for sound, Nat. Commun. **7**, 13368 (2016).

[14] L. J. Maczewsky, J. M. Zeuner, S. Nolte, and A. Szameit, Observation of photonic anomalous floquet topological insulators, Nat. Commun. **8**, 13756 (2017).

[15] S. Mukherjee, A. Spracklen, M. Valiente, E. Andersson, P. Öhberg, N. Goldman, and R. R. Thomson, Experimental observation of anomalous topological edge modes in a slowly driven photonic lattice, Nat. Commun. **8**, 13918 (2017).

[16] K. Wintersperger, C. Braun, F. N. Ünal, A. Eckardt, M. D. Liberto, N. Goldman, I. Bloch, and M. Aidelsburger, Realization of an anomalous floquet topological system with ultracold atoms, Nat. Phys. **16**, 1058 (2020).

[17] A. Lazarides, A. Das, and R. Moessner, Equilibrium states of generic quantum systems subject to periodic driving, Phys. Rev. E **90**, 012110 (2014).

[18] L. D'Alessio and M. Rigol, Long-time Behavior of Isolated Periodically Driven Interacting Lattice Systems, Phys. Rev. X **4**, 041048 (2014).

[19] P. Ponte, A. Chandran, Z. Papić, and D. A. Abanin, Periodically driven ergodic and many-body localized quantum systems, Ann. Phys. **353**, 196 (2015).

[20] H. Dehghani, T. Oka, and A. Mitra, Dissipative floquet topological systems, Phys. Rev. B **90**, 195429 (2014).

[21] T. Iadecola and C. Chamon, Floquet systems coupled to particle reservoirs, Phys. Rev. B **91**, 184301 (2015).

[22] T. Iadecola, T. Neupert, and C. Chamon, Occupation of topological floquet bands in open systems, Phys. Rev. B **91**, 235133 (2015).

[23] K. I. Seetharam, C.-E. Bardyn, N. H. Lindner, M. S. Rudner, and G. Refael, Controlled Population of Floquet-Bloch States

via Coupling to Bose and Fermi Baths, Phys. Rev. X **5**, 041050 (2015).
[24] E. Canovi, M. Kollar, and M. Eckstein, Stroboscopic prethermalization in weakly interacting periodically driven systems, Phys. Rev. E **93**, 012130 (2016).
[25] T. Mori, T. Kuwahara, and K. Saito, Rigorous Bound on Energy Absorption and Generic Relaxation in Periodically Driven Quantum Systems, Phys. Rev. Lett. **116**, 120401 (2016).
[26] T. Kuwahara, T. Mori, and K. Saito, Floquet–magnus theory and generic transient dynamics in periodically driven many-body quantum systems, Ann. Phys. **367**, 96 (2016).
[27] D. A. Abanin, W. D. Roeck, W. W. Ho, and F. Huveneers, Effective hamiltonians, prethermalization, and slow energy absorption in periodically driven many-body systems, Phys. Rev. B **95**, 014112 (2017).
[28] D. Abanin, W. D. Roeck, W. W. Ho, and F. Huveneers, A rigorous theory of many-body prethermalization for periodically driven and closed quantum systems, Commun. Math. Phys. **354**, 809 (2017).
[29] D. A. Abanin, E. Altman, I. Bloch, and M. Serbyn, Colloquium: Many-body localization, thermalization, and entanglement, Rev. Mod. Phys. **91**, 021001 (2019).
[30] L. Fleishman and P. W. Anderson, Interactions and the anderson transition, Phys. Rev. B **21**, 2366 (1980).
[31] L. D'Alessio and A. Polkovnikov, Many-body energy localization transition in periodically driven systems, Ann. Phys. **333**, 19 (2013).
[32] P. Ponte, Z. Papić, F. Huveneers, and D. A. Abanin, Many-Body Localization in Periodically Driven Systems, Phys. Rev. Lett. **114**, 140401 (2015).
[33] A. Lazarides, A. Das, and R. Moessner, Fate of Many-Body Localization Under Periodic Driving, Phys. Rev. Lett. **115**, 030402 (2015).
[34] J. Z. Imbrie, On many-body localization for quantum spin chains, J. Stat. Phys. **163**, 998 (2016).
[35] D. A. Abanin, W. De Roeck, and F. Huveneers, Theory of many-body localization in periodically driven systems, Ann. Phys. **372**, 1 (2016).
[36] V. Khemani, A. Lazarides, R. Moessner, and S. L. Sondhi, Phase Structure of Driven Quantum Systems, Phys. Rev. Lett. **116**, 250401 (2016).
[37] A. Agarwala and D. Sen, Effects of interactions on periodically driven dynamically localized systems, Phys. Rev. B **95**, 014305 (2017).
[38] P. W. Anderson, Absence of diffusion in certain random lattices, Phys. Rev. **109**, 1492 (1958).
[39] P. Sala, T. Rakovszky, R. Verresen, M. Knap, and F. Pollmann, Ergodicity Breaking Arising from Hilbert Space Fragmentation in Dipole-Conserving Hamiltonians, Phys. Rev. X **10**, 011047 (2020).
[40] S. Moudgalya, B. A. Bernevig, and N. Regnault, Quantum many-body scars and hilbert space fragmentation: A review of exact results, Rep. Prog. Phys. **85**, 086501 (2022).
[41] S. Moudgalya and O. I. Motrunich, Hilbert Space Fragmentation and Commutant Algebras, Phys. Rev. X **12**, 011050 (2022).
[42] V. Khemani, M. Hermele, and R. Nandkishore, Localization from hilbert space shattering: From theory to physical realizations, Phys. Rev. B **101**, 174204 (2020).
[43] C. J. Turner, A. A. Michailidis, D. A. Abanin, M. Serbyn, and Z. Papić, Weak ergodicity breaking from quantum many-body scars, Nat. Phys. **14**, 745 (2018).
[44] W. W. Ho, S. Choi, H. Pichler, and M. D. Lukin, Periodic Orbits, Entanglement, and Quantum Many-Body Scars in Constrained Models: Matrix Product State Approach, Phys. Rev. Lett. **122**, 040603 (2019).
[45] A. Kumar, P. T. Dumitrescu, and A. C. Potter, String order parameters for one-dimensional floquet symmetry protected topological phases, Phys. Rev. B **97**, 224302 (2018).
[46] A. J. Friedman, S. Gopalakrishnan, and R. Vasseur, Integrable Many-Body Quantum Floquet-Thouless Pumps, Phys. Rev. Lett. **123**, 170603 (2019).
[47] M. Ljubotina, L. Zadnik, and T. Prosen, Ballistic Spin Transport in a Periodically Driven Integrable Quantum System, Phys. Rev. Lett. **122**, 150605 (2019).
[48] L. Piroli, B. Bertini, J. I. Cirac, and T. Prosen, Exact dynamics in dual-unitary quantum circuits, Phys. Rev. B **101**, 094304 (2020).
[49] M. Lu, G. H. Reid, A. R. Fritsch, A. M. Piñeiro, and I. B. Spielman, Floquet Engineering Topological Dirac Bands, Phys. Rev. Lett. **129**, 040402 (2022).
[50] M. Wampler and I. Klich, Arrested development and fragmentation in strongly-interacting Floquet systems, SciPost Phys. **14**, 145 (2023).
[51] H. Cohen, *Number Theory*, *Graduate Texts in Mathematics*, 1st ed. (Springer, Berlin, 2005).
[52] S. Wolfram, Statistical mechanics of cellular automata, Rev. Mod. Phys. **55**, 601 (1983).
[53] M. Aizenman and S. Warzel, Localization bounds for multiparticle systems, Commun. Math. Phys. **290**, 903 (2009).
[54] J. Iaconis, S. Vijay, and R. Nandkishore, Anomalous subdiffusion from subsystem symmetries, Phys. Rev. B **100**, 214301 (2019).
[55] W. De Roeck and F. Huveneers, Stability and instability towards delocalization in many-body localization systems, Phys. Rev. B **95**, 155129 (2017).
[56] W. De Roeck and J. Z. Imbrie, Many-body localization: Stability and instability, Philos. Trans. R. Soc. A **375**, 20160422 (2017).
[57] I.-D. Potirniche, S. Banerjee, and E. Altman, Exploration of the stability of many-body localization in $d > 1$, Phys. Rev. B **99**, 205149 (2019).
[58] A. Morningstar, L. Colmenarez, V. Khemani, D. J. Luitz, and D. A. Huse, Avalanches and many-body resonances in many-body localized systems, Phys. Rev. B **105**, 174205 (2022).
[59] A. Nahum, S. Vijay, and J. Haah, Operator Spreading in Random Unitary Circuits, Phys. Rev. X **8**, 021014 (2018).
[60] H. Zhao, F. Mintert, R. Moessner, and J. Knolle, Random Multipolar Driving: Tunably Slow Heating through Spectral Engineering, Phys. Rev. Lett. **126**, 040601 (2021).
[61] H. Zhao, M. S. Rudner, R. Moessner, and J. Knolle, Anomalous random multipolar driven insulators, Phys. Rev. B **105**, 245119 (2022).
[62] M. Wampler, B. J. J. Khor, G. Refael, and I. Klich, Stirring by Staring: Measurement-Induced Chirality, Phys. Rev. X **12**, 031031 (2022).